Cement & Concrete Composites 37 (2013) 108–118

Contents lists available at SciVerse ScienceDirect

Cement & Concrete Composites

journal homepage: www.elsevier.com/locate/cemconcomp

Synthesis and characterization of red mud and rice husk ash-based geopolymer composites

Jian He [a], Yuxin Jie [b], Jianhong Zhang [b], Yuzhen Yu [b], Guoping Zhang [a,*]

[a] Department of Civil and Environmental Engineering, Louisiana State University, Baton Rouge, LA 70803, USA
[b] State Key Laboratory of Hydroscience and Engineering, Tsinghua University, Beijing 100084, China

ARTICLE INFO

Article history:
Received 4 January 2012
Received in revised form 26 November 2012
Accepted 28 November 2012
Available online 11 December 2012

Keywords:
Composite
Compressive strength
Geopolymer
Microstructure
Red mud
Rice husk ash

ABSTRACT

A new type of geopolymer composite was synthesized from two industrial wastes, red mud (RM) and rice husk ash (RHA), at varying mixing ratios of raw materials and the resulting products characterized by mechanical compression testing, X-ray diffraction, and scanning electron microscopy to assess their mechanical properties, microstructure, and geopolymerization reactions. Prolonged curing significantly increases the compressive strength and Young's modulus, but reduces the ductility. Higher RHA/RM ratios generally lead to higher strength, stiffness, and ductility, but excessive RHA may cause the opposite effect. The compressive strength ranges from 3.2 to 20.5 MPa for the synthesized geopolymers with nominal Si/Al ratios of 1.68–3.35. Microstructural and compositional analyses showed that the final products are mainly composed of amorphous geopolymer binder with both inherited and neoformed crystalline phases as fillers, rendering the composites very complex composition and highly variable mechanical properties. Uncertainties in the composition, microstructure, the extent of RHA dissolution, and side reactions may be potential barriers for the practical application of the RM–RHA based geopolymers as a construction material.

1. Introduction

Red mud (RM) is the major waste produced by the alumina refining industry where the Bayer process is used to extract alumina from bauxite ores [1]. This process involves using highly concentrated NaOH solution for the ore digestion at high pressures and elevated temperatures (e.g., 150–230 °C) [2]. As a result, fresh RM slurry is characterized by strong alkalinity (pH 10.5–13) and high water content [3]. These characteristics, together with its concentrated heavy metals and other trace elements (e.g., radionuclides), make beneficial reuse or proper disposal of RM difficult. The worldwide production of RM exceeds 120 million tons (MT) annually [1]. At present, because of stricter environmental concerns and regulations, direct offsite disposal of untreated or unprocessed RM slurry is prohibited [4]. Instead, fresh RM slurry is usually transported to waste lakes for impoundments, followed by dewatering and drying to reduce its volume and maintenance costs. However, such a disposal method is not sustainable and still poses potential threats to the environment and public health. Therefore, new trustworthy and environmentally friendly disposal methods are urgently needed. To date, although enormous efforts have been made on RM treatment, recycling, and utilization [5–9], an economical, widely accepted technology for the recycle and reuse of RM has yet to be developed.

Rice husk ash (RHA) is also an industrial waste produced by burning rice husk primarily for the generation of electricity, a kind of sustainable biomass energy. Rice husk, the hard protective shell of rice grains, is an agricultural by-product of rice mills. It is available in many regions of the world, particularly in under-developed countries. It consists of approximately 40 wt.% cellulose, 30 wt.% lignin, and 20 wt.% silica [10,11]. It is one of the most intractable agricultural wastes known to man, because its tough, woody, and abrasive nature along with a high silica content makes its proper disposal very difficult [12,13]. The growing environmental concerns and need for energy from renewable biomass have led to a useful and economical solution—burning rice husk for electricity generation with net zero carbon output to the atmosphere. After burning, the residual ash is known as RHA. The main component of the ash is silica (>90–95 wt.%), existing predominantly in amorphous and partly in crystalline phases (although the temperature and duration of burning affect the ratio of amorphous to crystalline phases of silica) [12], with residual carbon as the major impurity and other trace elements such as K and Ca. In general, after burning off organic constituents of the rice husk, RHA consists of highly porous particles, leading to a low bulk unit weight and a very high external surface area [14]. The amorphous silica in RHA is reactive and can be used as a pozzolana. To date, RHA has been successfully

* Corresponding author. Tel.: +1 225 578 6047; fax: +1 225 578 4945.
E-mail addresses: gzhang@lsu.edu, gzhang@alum.mit.edu (G. Zhang).

0958-9465/$ - see front matter © 2012 Elsevier Ltd. All rights reserved.
http://dx.doi.org/10.1016/j.cemconcomp.2012.11.010

used in concrete for reduced permeability and enhanced sulfate resistance [10,11]. In addition, it has also been used to partially replace fly ash to regulate the Si/Al ratio in geopolymers [15], among other applications [16].

Compared with other biomass fuels, rice husk is unusually high in ash content, about 20%, which is influenced by the rice's variety, climatic condition, and geographical location [17,18]. According to a 2003 RHA market study, the annual rice husk production totals approximately 120 MT. As such, about 24 MT of RHA was generated annually by the biomass energy industry. Da Costa et al. [19] stated that the most common method of RHA disposal is dumping on waste land, thus creating an environmental hazard through pollution and land dereliction problems. Therefore, cost-effective and environmentally friendly technologies for RHA disposal are also urgently needed due to the immerse amount of RHA generated annually.

The geopolymer technology has recently attracted increasing attention as a viable solution to reusing and recycling industrial solid wastes and by-products, which provides a sustainable and cost-effective development for many problems where hazardous residues have to be treated and stored under critical environmental conditions [20]. This innovative technology may also be harnessed to resolve the economic and environmental challenges faced by the RM and RHA-producing industries. Geopolymerization is to react amorphous silica-rich and alumina-rich materials (usually as finely divided powders) with a high alkaline solution to form amorphous to semi-crystalline aluminosilicate polymers, where Si^{4+} and Al^{3+} cations in the framework of geopolymer binders are tetrahedrally coordinated and linked by oxygen bridges. According to the literature, geopolymerization is a complex process, which may be roughly divided into the following steps [21–24]: (1) the dissolution of amorphous phases by alkali solution; (2) transport, orientation, and condensation of precursor ions into monomers; (3) polycondensation and polymerization of monomers into amorphous to semi-crystalline aluminosilicate polymers. The resulting geopolymers are members of the inorganic polymer family, which generally exhibit excellent physical and chemical properties and hence may readily be used in diverse applications, such as insulation material, cementitious material, and waste fixation. Their chemical composition is similar to that of natural zeolitic materials, but they are usually amorphous instead of crystalline [25,26].

Generally, materials containing mostly amorphous silica (SiO_2) and alumina (Al_2O_3) are a possible source for geopolymer production. In fact, a great number of minerals and industrial byproducts have been studied as raw materials for geopolymer synthesis, including pozzolana [27,28], natural aluminosilicate minerals [26], metakaolin [22,23,29–31], fly ash [32,33], granulated blast furnace slag [34,35], fly ash and kaolinite mixture [36], fly ash and metakaolin mixture [37,38], RM and metakaolin mixture [4], and RM and fly ash mixture [1]. More importantly, the starting raw materials play a significant role in the geopolymer reaction and affect the mechanical properties and microstructure of the final geopolymeric products [1,23,39]. Therefore, one of the primary research efforts in the past has been devoted to identify different source materials for geopolymer production and to characterize the properties of the geopolymeric products for potential practical applications.

This paper presents an experimental study on the synthesis and characterization of a new type of geopolymer composite derived from two industrial wastes, RM and RHA, with extra NaOH added at a measurable quantity. It is a further advancement of the authors' previous work on the RM and fly ash-based geopolymers, whose synthesis required the activator, Na-silicate or Na-trisilicate solution [1]. Because the RHA is a good source of reactive amorphous silica, this study aimed to eliminate the use of Na-silicate or Na-trisilicate solution that is usually required for geopolymer synthesis. Instead, the RHA dissolved in NaOH solution was used as an economical alternative to Na-silicate. Moreover, the geopolymer synthesis developed in this study took full advantages of the starting raw materials: dissolved NaOH and alumina (Al_2O_3) in the RM and amorphous silica (SiO_2) in the RHA. The only non-waste raw material used in this study was sodium hydroxide (NaOH), which was expected to enhance the alkalinity for a higher degree of geopolymerization. Therefore, the main objectives of this paper are twofold: (1) to investigate the potential utilization of the RM and RHA as raw materials for geopolymer production, and (2) to characterize the composition, microstructure, and mechanical properties of the resulting geopolymer products. This study intends to convert two industrial wastes into a cementitious composite as a beneficial construction material and hence to develop a potentially viable technology for the utilization of the RM and RHA via geopolymerization. As discussed below, because both geopolymer binder and inactive fillers are present, the final products are geopolymer composites.

2. Materials and methods

2.1. Materials

The raw materials used for geopolymer synthesis include RM slurry (Noranda Alumina LLC, USA), RHA (Agrilectric Research Co., USA), sodium hydroxide (purity quotient: 99%, Sigma–Aldrich Co., USA), and deionized water. The original, highly diluted RM slurry obtained directly from the alumina refining plant has a pH 11.9 and contains mainly water with dissolved Na-aluminate ($NaAlO_2$) and sodium hydroxide (NaOH) as the liquid phase, and hematite (Fe_2O_3) and alumina (Al_2O_3) as the solid phases (Table 1), as well as other trace phases (e.g., calcite), which were identified by the X-ray diffraction (XRD) analysis discussed below. Silica is nearly absent, because the Bayer process essentially removes all silica prior to alumina extraction. To better control the synthesis process, facilitate geopolymerization reaction, and minimize the influence of compositional variation on the end products, the as-received slurry was air-dried, homogenized, and pulverized until all solids passed a #60-mesh (250 μm opening) sieve.

Two as-received RHA samples with different gradations were used without additional processing: a regular RHA sample consisted of particles of a wider size range, while the other one was pre-ground to finer sizes by passing all particles through a #100-mesh (150 μm opening) sieve. They are denoted hereafter by RHA and RHA(f), respectively. The chemical composition of the RHA is also summarized in Table 1. As indicated by the XRD analysis discussed later, the silica in the RHA is mainly amorphous. It is worth noting that the RAH also contains 6 wt.% of residual carbon.

Table 1
Size fraction (wt.%) and chemical composition (wt.%) of the RM and RHA samples.

Composition	RM	RHA
Clay (⩽2 μm)	33.0	4.0
Silt (2–75 μm)	43.0	86.5
Sand (>75 μm)	24.0	9.5
SiO_2	1.2	91.5
Al_2O_3	14.0	–
Fe_2O_3	30.9	–
NaOH	20.2	–
$NaAlO_2$	23.0	–
CaO	2.5	–
K_2O	–	2.3
TiO_2	4.5	–
MnO	1.7	–
C	–	6.0
Total	98.0	99.8

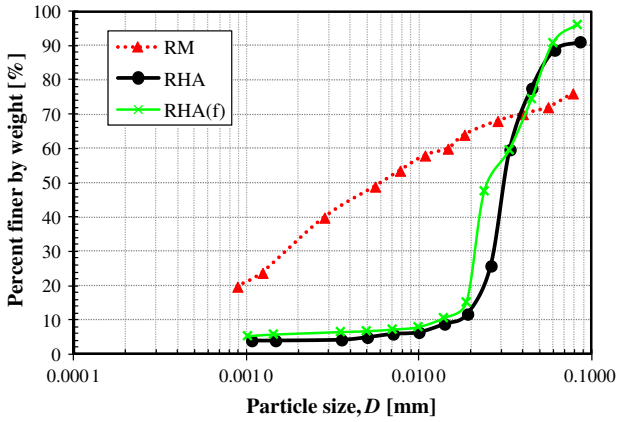

Fig. 1. Particle size distribution curves of the RM powder and the two RHA samples.

Because of the low density of carbon, the volumetric percentage is much greater than 6%. As such, the RHA has a gray to blackish color.

Fig. 1 shows the particle size distribution (PSD) curves of the two RHA and pre-processed RM determined by the standard test method [40]. The mean particle size (D_{50}) is 6, 32, and 25 μm for the RM, RHA, and RHA(f), respectively. It is noteworthy that the highly porous nature of the RHA particles affects the settling velocity due to the creeping flow through the pores, the RHA's PSD obtained by the conventional hydrometer method may deviate from the true particle sizes. In addition, the specific gravity of RM and RHA determined by the standard test method [40] is 3.94 and 2.06, respectively. The higher specific gravity of RM is caused by the presence of hematite with a specific gravity of 5.3, while the presence of carbon in the RHA significantly lower its specific gravity. Moreover, the RM is a non-calcined material, while the RHA a calcined one.

2.2. Geopolymer synthesis

The synthesis process started with mixing the two dry powders at a pre-designed RHA to RM weight ratio (RHA/RM), followed by adding NaOH solution with a pre-designed concentration to the powder mixture at a solution to solid weight ratio of 1.2. Then the mixture was blended by a magnetic stirring bar for at least 15 min to ensure sufficient reaction (i.e., mainly the dissolution of reactive phases) between the powder and NaOH solution, resulting in the formation of a geopolymer precursor with a slurry to paste consistency. To prepare geopolymer specimens for subsequent mechanical and microstructural characterization, the precursor was then poured into cylindrical molds with an inner diameter of 2 cm and height of 5 cm (i.e., an aspect ratio of 2.5 to minimize the end effects during unconfined compression testing), followed by curing in a laboratory ambient environment (e.g., room temperature and atmospheric pressure) for 14 days. The specimens were then demolded, followed by prolonged curing in exposed conditions. To ensure reproducibility, three duplicate specimens were prepared for each geopolymer composition. Finally, although curing at elevated temperatures can reduce the curing time and enhance the mechanical properties of the final cured products, this option was not examined in this study owing to the difficulty of high temperature curing in engineering practice.

To examine the compositional influence on geopolymer properties, several parameters were varied during synthesis. The pre-designed composition (e.g., Si/Al and Na/Si ratios) of the geopolymer specimens controls the quantity of each raw material or chemical used in each synthesis. Excluding a fixed NaOH solution to solid weight ratio of 1.2, totally four sets of synthesis parameters were investigated in this study: (A) the curing duration varied from 14 to 49 days with an interval of 7 days for the geopolymer with an RHA/RM ratio of 0.4 and a NaOH concentration of 4 M; (B) the RHA/RM ratio, which essentially controls the Si/Al ratio of the end product, varied from 0.3, 0.4, 0.5, to 0.6; (C) the alkalinity or Na/Si ratio was altered by changing the concentration of NaOH solutions (i.e., 2, 4, and 6 M); and (D) the RHA gradation (i.e., a regular vs. a finer RHA). Table 2 summarizes the various synthesis parameters and their purposes for each of the four test sets. To clearly determine the influence of each specific parameter and isolate the influence of other different synthesis parameters, only the selected parameter was altered within each test set, while others were kept constant.

2.3. Mechanical and microstructural characterization

Unconfined compression tests [40] were performed on cured cylindrical specimens using an automated GeoTAC loading frame (*Trautwein* Soil Testing Equipment, Inc., USA) at a fixed strain rate of 0.5%/min. The two ends of each specimen were polished by sand paper to obtain flat and parallel surfaces. A very thin layer of lubricant coating was applied to the two ends of each specimen, in order to minimize the friction and hence shear stress development between the specimen end surface and polished stainless steel end platens of the loading frame.

Chemical and microstructural characterization of the two raw materials and resulting geopolymers were also performed to enhance the understanding of the composition—microstructure—strength relationship. The mineralogical composition of the RM, RHA, and completely cured RM–RHA geopolymer was characterized by X-ray diffraction (XRD) using a Bruker/Siemens D5000 automated X-ray powder diffractometer. All XRD scans used Cu Kα radiation, a step size of 0.02°, a scan speed of 0.02° per 2 s, and a scan range of 2–42° 2θ (diffraction angle). For the cured geopolymer, the powdery sample for XRD analysis was obtained by wet grinding with alcohol in a McCrone micronizing mill (McCrone Accessories and Components, USA) for 3 min, which usually generates a fine powder with particle sizes $\leqslant$38 μm for most silicate minerals. The particle micromorphology of the RHA and RM and the microstructure of the cured geopolymers were examined using an FEI Quanta 200 scanning electron microscope (SEM) at an accelerating voltage of 20 kV. Chemical elemental analyses were also performed by an EDAX energy-dispersive X-ray spectroscopy (EDXS) device equipped with the SEM system. For the microstructure of the RM–RHA geopolymer, small pieces selected from the cylindrical specimens loaded to failure by unconfined compression

Table 2
Summary of the varied synthesis parameters and their purposes.

Test set	The parameter varied	Purpose	Other fixed parameters
A	Curing duration = 14, 21, 28, 35, 42, 49 days	Time for complete curing	Solution to solid weight ratio = 1.2
B	RHA/RM weight ratio = 0.3, 0.4, 0.5, 0.6	Effect of Si/Al ratio	RHA/RM weight ratio = 0.4
C	Concentration of NaOH solution = 2, 4, 6 M	Effect of alkalinity	Curing duration = 60 days
D	RHA gradation = regular and finer RHA	Effect of RHA particle sizes	NaOH solution concentration = 4 M RHA gradation = regular RHA

testing were examined, with a particular attention to the fractured failure surface. The external surfaces of the geopolymer samples were avoided, because their aerial exposure during curing may lead to the formation of different microstructure that is not representative of the entire geopolymer specimen. All examined samples were coated by platinum for subsequent SEM and EDXS analyses.

3. Results and discussion

3.1. Effect of curing time

Fig. 2 shows the evolution of stress–strain curves with curing time for the RM–RHA geopolymers prepared in Test Set A (Table 2), where the compressive strength (σ_f), Young's modulus (E), and failure strain (ε_f) can be obtained and compared (Table 3). It is clear that both the σ_f and E increase with curing time. However, the σ_f stabilizes at a nearly constant value of 11.7 MPa after 35 days of curing, suggesting that the geopolymer sample can achieve complete curing in about 35 days. Moreover, with curing progressing, there is an obvious transition from a more ductile to a brittle failure. In fact, the ε_f decreases continuously. If the stabilization of peak strength is adopted as a criterion to judge whether curing is complete, then some geopolymerization or side reactions may still occur after complete curing, as indicated by the continuous increase in stiffness or decrease in failure strain while under a constant peak strength. To summarize, this set of tests suggests that the strength, Young's modulus, and failure strain of completely cured RM–RHA geopolymers are 11.7 MPa, 1.77 GPa, and 0.75%, respectively. These results also demonstrate that curing is critical in the development of mechanical properties of this type of geopolymers. Therefore, to ensure complete curing and minimize the undesired influence of incomplete curing on the interpretation of results, other geopolymer samples discussed in the following sections were all cured for 60 days before they were examined under unconfined compression testing.

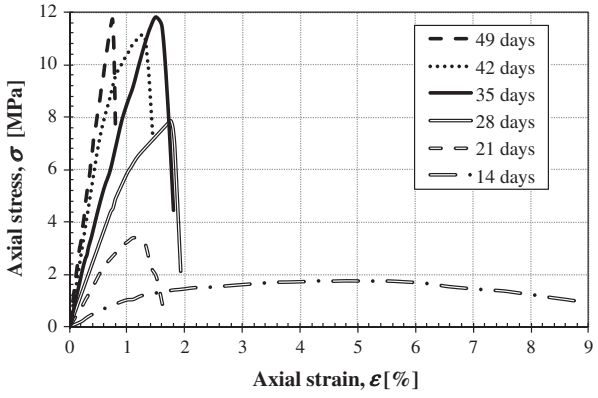

Fig. 2. Influence of curing duration on the stress–strain behavior of the RM–RHA geopolymer.

Table 3
Summary of the mechanical properties of the RM–RHA geopolymers.

Test set	Varied synthesis parameter	Compressive strength σ_f (MPa)	Failure strain ε_f (%)	Young's modulus E (GPa)
A	49 Days	11.70	0.75	1.77
	42 Days	11.13	1.30	1.39
	35 Days	11.82	1.50	0.99
	28 Days	7.86	1.75	0.62
	21 Days	3.40	1.10	0.37
	14 Days	1.74	4.80	0.1
B	RHA/RM = 0.6	11.86	0.91	1.34
	RHA/RM = 0.5	20.46	1.13	1.89
	RHA/RM = 0.4	11.70	0.75	1.77
	RHA/RM = 0.3	3.16	0.54	0.76
C	NaOH 6 M	8.23	1.02	0.90
	NaOH 4 M	11.70	0.75	1.77
	NaOH 2 M	15.23	2.62	0.89
D	Regular RHA	11.70	0.75	1.77
	Finer RHA	16.08	0.91	2.03

It is noteworthy that the complete curing time of 35 days is considerably longer than that of the geopolymers derived from other raw materials such as metakaolin, fly ash, or furnace slag. For instance, He et al. [29] reported that a duration of 14 days was required for the complete curing of a metakaolin-based geopolymer, and Zhang et al. [1] pointed out that 28 days were required for the complete curing of a RM and fly ash-based geopolymer. In general, calcined materials that typically have finer gradation possess higher reactivity, since most crystalline phases in the pre-calcined materials collapse their structure and become amorphous after calcination at high temperatures [41]. For this study, the RM is non-calcined and is dominated by crystalline phases (as confirmed by the XRD results below) that are non-reactive and present as inactive fillers in the end products. The slow rate of geopolymerization is mainly caused by the relative large particles of the RHA (Table 1) that reduce the rate of dissolution in an alkali solution. As a result, much longer reaction or curing time is required for this type of RM–RHA based geopolymers to develop its maximum strength and stiffness. In addition, as validated by the XRD results, a great amount of impurities (e.g., crystalline phases, unreacted amorphous phases) in the final geopolymeric products from the two raw materials may cause negative impact on the geopolymerization rate.

3.2. Effect of raw material mix ratio

Fig. 3 presents the influence of varied raw material mix ratios (i.e., RHA/RM weight ratios = 0.3, 0.4, 0.5, 0.6) on the mechanical properties of the RM–RHA geopolymers (i.e., Test Set B in Table 2). The change in the RHA/RM ratio results in variable Si/Al ratios. Based on the chemical composition (Table 1), the corresponding nominal Si/Al ratios are 1.68, 2.24, 2.80, and 3.35 for the chosen RHA/RM. According to Fig. 3, the σ_f, E, and ε_f are all enhanced while the Si/Al ratio increases from 1.68 to 2.80. Specifically, the σ_f is in the range of 3.2–20.5 MPa (Table 3). Such improvements can be explained by two possible reasons: (a) an increased amount of reactive silica from the RHA results in a higher density of the Si–O–Si bonds in the geopolymer, leading to a higher strength and

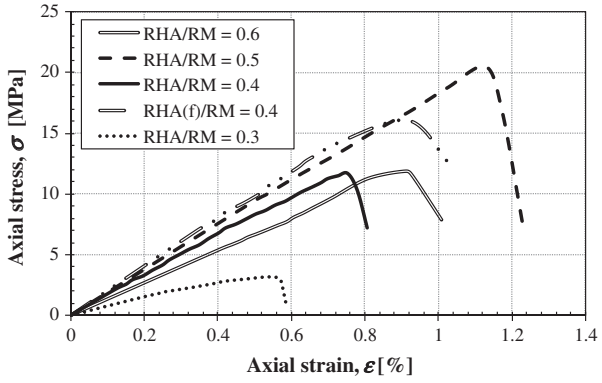

Fig. 3. Influence of the RHA/RM weight ratio and RHA particle size on the mechanical properties of the RM–RHA geopolymer.

stiffness; and (b) a higher amount of RHA with a high specific surface area makes the end products more ductile.

However, all of these parameters (i.e., σ_f, E, and ε_f) decrease when the Si/Al ratio changes from 2.80 to 3.35 (Table 3). Theoretically, the Si–O–Si bonds are stronger than those of Si–O–Al and Al–O–Al [42], implying that the strength of geopolymers should increase with the Si/Al ratio because the density of the Si–O–Si bonds increases with the Si/Al ratio [43]. However, in this study, contrary to the aforementioned principle, the geopolymers with a higher Si/Al ratio (i.e., 3.35) exhibit poorer mechanical properties, suggesting that other synthesis parameters begin to affect the mechanical properties [43]. The critical reasons for this phenomenon are believed to include: (a) relatively larger RHA solid particles cause negative influence on the rate and extent of geopolymerization reaction [44], which is more dominant when the RHA makes up a higher fraction in the raw material mix. As such, the resulting geopolymers are weaker; (b) a higher proportion of RHA results in more unreacted RHA (as observed by the SEM analysis) in the end products, whose poor mechanical properties make the final geopolymeric products weaker and less ductile; and (c) a higher concentration of soluble Si hinders the reorganization of Si and Al, and hence results in a reduced skeletal density of the geopolymer binder [43], which also makes the geopolymers weaker.

3.3. Effect of the RHA particle size

Fig. 3 also includes the stress–strain curve for the geopolymer synthesized with a finer RHA sample that was ground to pass a #100 mesh (i.e., Test Set D in Table 2). As expected, this sample possesses improved σ_f, E, and ε_f than the one derived from a regular RHA and the same RHA/RM ratio (Fig. 3 and Table 3). There are two reasons for such improvements: (a) finer particle sizes improve the reactivity of the RHA so that a higher degree of geopolymerization of the raw materials can be achieved [44], which makes the resulting geopolymer specimens stronger and more ductile; and (b) the higher specific surface area of finer RHA particles also results in stronger and more ductile geopolymers [45]. Therefore, the mechanical properties (i.e., σ_f, E, and ε_f) of the final geopolymer products are highly dependent upon the physical properties, such as particle size, of the raw materials, in addition to their chemical compositions such as the Si/Al ratio.

3.4. Influence of alkali concentration

Fig. 4 shows the influence of NaOH concentration on the stress–strain curves of the RM–RHA geopolymer (i.e., Test Set C in Table 2). Clearly, different mechanical properties resulting from varied NaOH concentrations (2, 4, and 6 M) can be identified. That is, the σ_f decreases with increasing NaOH concentration, while the E and ε_f either decrease or increase (Table 3). It is commonly agreed that alkalinity is one of the most significant factors affecting the properties of geopolymers since they are alkali-activated materials [1,33,44,46]. In this study, however, it appears that alkali concentration may cause variable mechanical behavior, which differs from some previous observations that higher alkalinity yields geopolymers with higher compressive strength and stiffness [47]. The possible reasons accounting for this include: (1) the higher viscosity of higher NaOH concentration solutions hinders the leaching of silicon and aluminum, resulting in a negative effect on the degree of geopolymerization reaction [44] and hence the mechanical properties of the final products; (2) the excess OH^- concentration from higher NaOH concentration solutions causes aluminosilicate gel precipitation at very early stage [48], and consequently geopolymerization is hindered, resulting in detrimental influence on the mechanical properties [46]; and (3) as discussed later, the RHA's incomplete dissolution and reaction is believed to cause significant variability in mechanical properties of the final products. Therefore, NaOH concentration is also critical in affecting the mechanical properties of geopolymers.

3.5. X-ray diffraction (XRD) analysis

Fig. 5 shows the XRD patterns of the RM, RHA, and cured RM–RHA geopolymer. The sharp peaks in RM are mainly caused by the presence of hematite and calcite. The absence of discernible broad humps in the RM pattern indicates that the amorphous phases are absent or not present at large quantities. It is worth noting that, although the RM contains alumina (Al_2O_3) as indicated by the chemical analysis (Table 1), no alumina peaks are identified in the XRD pattern, suggesting that the alumina in the RM mainly presents as an amorphous phase. Thus, the RM provides mainly NaOH and Al either in the form of amorphous Al_2O_3 or dissolved $NaAlO_2$, but little Si, for geopolymerization. The RHA pattern has one sharp peak superimposed on a broad hump at 10–35° 2θ. The sharp peak is from cristobalite, a high-temperature polymorph of silica. The very broad hump is from amorphous silica, a major constituent in RHA [49–51]. A very weak peak from quartz, a crystalline phase of silica, is also present, but its height is masked by the broad hump from the amorphous silica. According to its chemical composition (Table 1), silica in the RHA is mainly present as amorphous phase with cristobalite [50] and trace crystalline quartz. This is in agreement with the general literature [12–14,51]. The above results agree well with the fact that RM is a non-calcined material consisting of mainly crystalline phases,

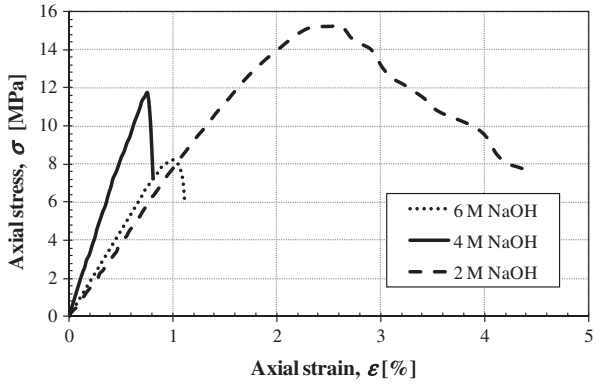

Fig. 4. Influence of the NaOH concentration on the mechanical properties of the RM–RHA geopolymers.

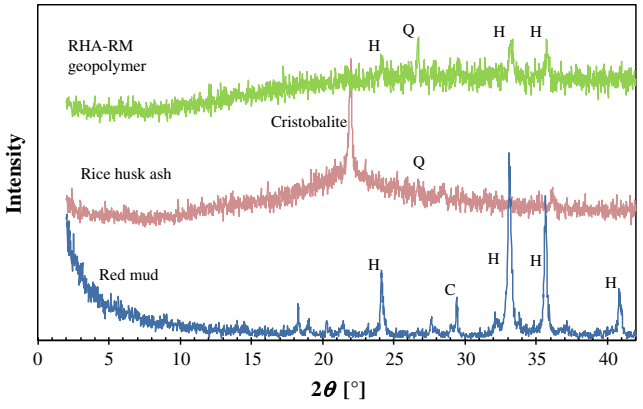

Fig. 5. XRD patterns of the RM, RHA, and RHA–RM geopolymer (H = hematite, C = calcite, Q = quartz).

while RHA is a calcined material with the majority of its crystalline phases converted to amorphous after high-temperature calcination [41].

In the RM–RHA geopolymer pattern, a large, broad, and non-symmetrical hump from amorphous phase is clearly observed at 15–35° 2θ, along with a few sharp peaks identified as crystalline hematite and quartz. This very broad hump may result from the superposition of two amorphous or semi-crystalline phases: (1) the residual reactive amorphous silica that is inherited from the RHA and spans from 15 to 35° 2θ, because incomplete dissolution and reaction may have taken place during geopolymerization [52], and (2) the amorphous geopolymer that is neoformed and usually spans from 18 to 35° 2θ. This observation also agrees well with the current understanding that geopolymers are amorphous to semi-crystalline aluminosilicates [22,23,29,52]. The presence of sharp peaks of hematite and quartz, inherited from the RM and RHA, respectively, suggests that crystalline phases are not involved in geopolymerization, but simply present as nonreactive fillers in the geopolymer binder [1,20,53]. Finally, some crystalline minerals such as quartz and calcite identified in the parent materials are not observed in the geopolymer. The possible reasons include: (a) they are not detectable or identifiable due to their very low concentrations in the final geopolymeric products; and (b) they may have participated in other side reactions during geopolymerization. For instance, calcium is known to react strongly with silica in the presence of alkali to form various phases of calcium silicate hydrate [23].

3.6. Characterization of microstructure

Fig. 6 shows the micromorphological features of the two raw materials. The RM (which was dried and ground to pass a #60 mesh sieve) is characterized by irregularly shaped aggregates that appear to be porous and comprised of much smaller particles (Fig. 6a and b). In fact, hematite, the major solid constituent of the RM, is finely-divided nanocrystals with a size of 20–50 nm [54]. Thus the aggregates are most likely hematite particles. Moreover, some observable needle-shaped particles (Fig. 6b), probably gypsum, show the existence of some impurities. The regular RHA particles are much more variable in size (e.g., 1–400 μm), and most of them have a thin shell or plate like shape. Interestingly, the surface of these shell fragments of the RHA particles has rectangular indents (Fig. 6c), which are believed to be inherited from the original structure of rice husk. Such a thin shell particle shape renders RHA a very high specific surface area. Fig. 6d shows a closer view of an RHA particle. Knowing the micromorphology of the RM and RHA can help identify whether some phases (e.g., nonreactive or unreacted reactive phases) in the final products are inherited from the parent materials. In addition, EDXS chemical analyses of these two materials (results are not shown) also confirm the above mineralogical analyses by XRD (Fig. 5) and their elemental compositions (Table 1).

Fig. 7 shows the microstructure of a representative fractured surface from a failed RM–RHA geopolymer specimen, along with the EDXS spectra of selected interesting spots. A porous and inhomogeneous microstructure with micro cracks and micro voids is clearly observed on this surface (Fig. 7a). These cracks may have two possible origins: (1) shrinkage cracks during geopolymer curing when water evaporation takes place; (2) load-induced cracks caused by the unconfined compression testing. On the other hand, the voids may be induced by another two reasons: (1) the residual air bubbles that are introduced into the geopolymer precursor through initial mixing; (2) the space that was initially occupied by water and then left as a void after water evaporation. Both

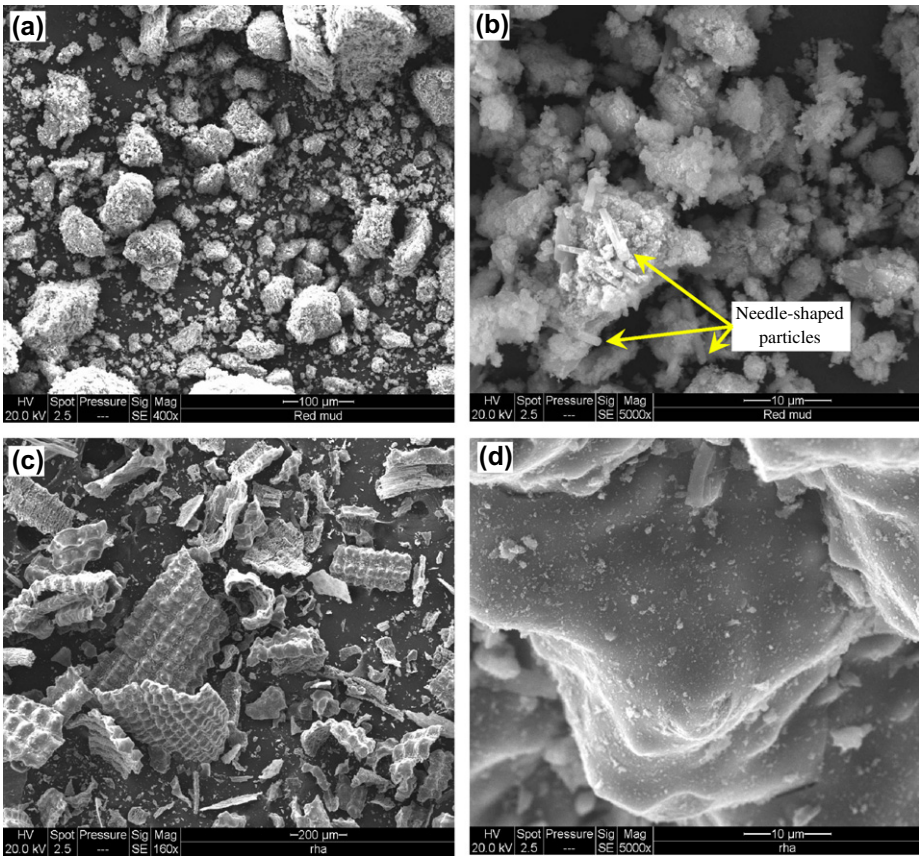

Fig. 6. SEM micrographs of the two raw materials: (a and b) RM; (c and d) RHA.

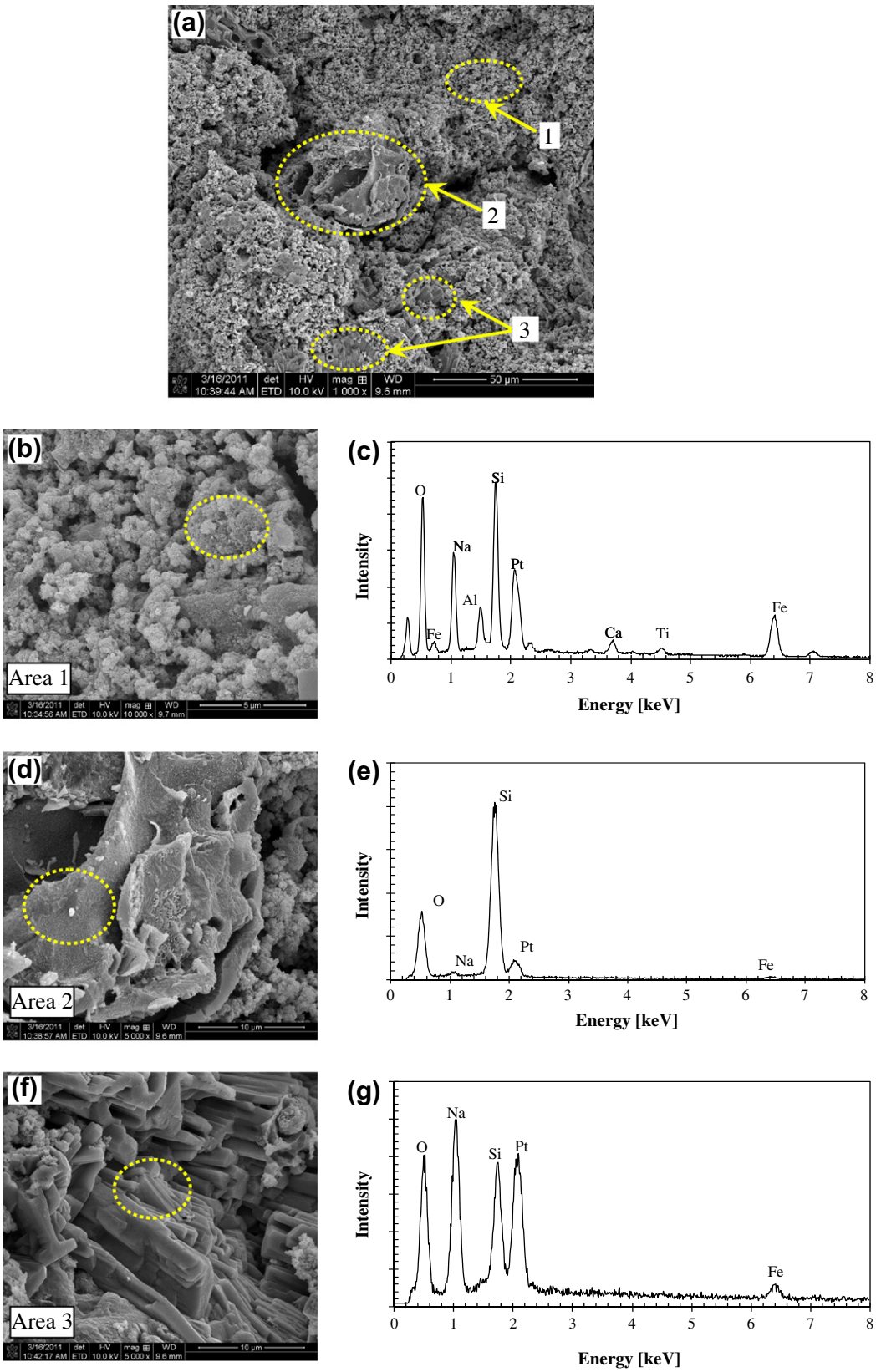

Fig. 7. SEM micrographs and EDXS analyses of the RM–RHA geopolymer: (a) a typical internal surface; (b) Area 1 in (a); (c) EDXS spectrum of a selected spot indicated by a circle in (d); (d) Area 2 in (a); (e) EDXS spectrum of a selected spot indicated by a circle in (d); (f) Area 3 in (a); and (g) EDXS spectrum of a selected spot indicated by a circle in (f).

cracks and voids have a significant detrimental influence on the strength of the geopolymer specimens. This agrees with the current understanding that special processing technology (e.g., using vacuum to remove air or high pressure to suppress air bubbles) can absolutely improve the geopolymer's mechanical properties (e.g., [55]).

Fig. 7b shows a magnified view of the microstructure of Area 1 indicated in Fig. 7a, while Fig. 7c is the EDXS spectrum obtained from the spot indicated by a circle in Fig. 7b. This area is also porous and filled with grains of 1–3 μm in size. Beneath these grains is a more bulky, continuous base. From the EDXS spectrum (Fig. 7c), this area mainly contains Na, Al, Si, O, and Fe. The former four elements are the major constituents of pure geopolymers. Therefore, the micro grains are likely hematite aggregates, while the bulky base is the geopolymer binder. In addition, the raw materials, particularly the RM, contain a considerable amount of impurities, which are also expected in the final products. This is clearly shown by the EDXS spectrum, where Fe, Ca, and Ti are also present. These impurities can influence to some extent the geopolymerization process [23]. In fact, this is a very important factor that causes the properties of the RM–RHA geopolymer to be variable and complicated.

Fig. 7d shows a magnified view of the microstructure of Area 2 indicated in Fig. 7a, while Fig. 7e the EDXS spectrum obtained from the spot indicated by a circle in Fig. 7d. The curved, shell-like appearance suggests that this observed particle of >30 μm in size is probably an RHA grain. The EDXS analysis further validates this observation, because only O and Si with trace Na and Fe are detected (Fig. 7e). Previous studies had similar observations that some unreacted source materials were still present as inclusions in the final products [33,56,57]. The amorphous RHA particle is relatively weak and thus can be considered as a defect in the geopolymer binder phase, resulting in some negative effects on the strength of the end products. This effect of course depends upon the quantity of the unreacted materials. In other words, the more the unreacted RHA in the final products, the lower the mechanical strength. This also explains the reason why increasing the Si/Al ratio from 2.8 to 3.35 (equivalent to the RHA/RM ratio from 0.5 to 0.6, respectively) causes negative effects on the mechanical performance (Fig. 3), because some excessive RHA particles may remain unreacted. To improve their mechanical properties, efforts should be made to assure the complete dissolution of the RHA in the geopolymer synthesis. This is why a longer duration of mixing (i.e., >15 min stirring) between the dry powder mixture and NaOH solution was employed in this study, as Rattanasak and Chindaprasirt [33] reported that longer duration of mixing increases the dissolution of raw materials.

Fig. 7f shows some prism-shaped, crystal-like particles observed in Area 3 in Fig. 7a. In fact, these particles were found to be distributed widely in the RM–RHA geopolymer composite. Their EDXS spectrum (Fig. 7g) shows the presence of Na, O, and Si, with trace Fe, suggesting that these prism particles are a certain form (e.g., Na_2SiO_3 or other forms) of sodium silicates derived from the side reaction of NaOH and RHA. This constituent is actually an impurity, which also influences negatively the mechanical properties of the final products. In particular, more sodium silicate is expected when the NaOH concentration is higher. As such, this agrees well with the aforementioned compressive strengths obtained from samples prepared with variable NaOH concentrations (Fig. 4). In fact, side reaction is also an important factor causing the significant variability in the mechanical behavior of geopolymers [23]. Owing to the complex chemical compositions of the RM and RHA, some side reactions are expected during geopolymerization reactions, which makes difficult the evaluation of the mechanical properties of final products.

3.7. Geopolymerization of RM and RHA

In this study, the RM, RHA, and NaOH are actually the three parent materials used for the synthesis of the RM–RHA geopolymers. Generally, sodium silicate solution is required as an activator for geopolymer synthesis, but it was not used in this study. Here a novelty is that the RHA consisting of mainly amorphous SiO_2 is used as an alternative or replacement activator. Zhang et al. [1] stated that the addition of sodium silicate in addition to NaOH may have positive influence on the compressive strength of the resulting geopolymers. A subsequent study that investigates the influence of addition of sodium silicate to the synthesis of the RM–RHA geopolymers is to be performed. On the basis of the XRD analysis, only amorphous phases in raw materials participate in the geopolymerization reactions. Thus, reactive phases for geopolymerization include: NaOH, dissolved alumina (Al_2O_3), and $NaAlO_2$ from the RM; amorphous SiO_2 from the RHA; and NaOH from the solution. Furthermore, as suggested by the XRD and SEM-EDXS results, most crystalline phases and some unreacted reactive phases in the parent materials are present as inactive fillers in the final geopolymeric products, which cause noticeably influences on the mechanical properties. Therefore, the RHA–RM geopolymers are a kind of composites containing the pure geopolymer binder and inactive fillers. In this regard, the nominal Si/Al ratios calculated based on the elemental composition (Table 1) of the parent materials reflect the total Si and Al ratios in the final composites, but not the true Si/Al ratios in the pure geopolymer binders, which should be less than the nominal values.

3.8. Factors affecting the mechanical performance of the final composites

It is well known that the starting materials play an important role in affecting the properties of final geopolymeric products. The properties of the RM–RHA geopolymer composites may vary significantly, because the raw materials (i.e., RM and RHA) are industrial wastes with impurities and variable chemical compositions. For instance, the properties of the RHA are firmly associated with the variety, climatic condition, and geographical location of rice paddy and the combustion conditions such as burning duration and burning temperature [12,14]. The properties of RM are also expected to be variable, depending upon the composition of the ores (e.g., bauxite) and processing conditions. Moreover, van Jaarsveld et al. [58] reported that the use of fly ashes (another industrial waste) of superficially similar composition but from different sources, as well as different batches of fly ash from the same source, was observed to result in geopolymers with notably different strengths. Therefore, industrial wastes as raw materials can seriously cause great variability in the properties of the final geopolymers. Further work is warranted to investigate how to minimize this negative influence induced by variations of the industrial wastes.

The mechanical properties of the RHA–RM geopolymer composites are complex and are affected by a wide array of synthesis parameters, including properties of the raw materials, extent and degree of geopolymerization of source materials, the chemical composition (e.g., Si/Al ratio) of the geopolymer binder, the relative fractions of geopolymer binder and inactive fillers, inactive fillers characteristics (e.g., particle size, shape, and strength), porosity and density, impurity elements (e.g., Ca, Mg, Fe), and associated side reactions. In addition, as pointed out above, the same parameters in determining the properties of geopolymeric products have changeable weight at different conditions. Thus, production of a consistent geopolymeric product with desirable properties from the RM and RHA requires a deeper understanding of the effects of all these factors on the properties of geopolymers formed under variable synthesis conditions.

3.9. Potential applications in practice

Although synthesizing geopolymers with the mixture of RM and RHA has never been reported in the literature, many researchers

have made efforts to synthesize geopolymers with other similar raw materials, such as the RM and metakaolin mixture [4], RM and fly ash mixture [1]. According to the literature, the σ_f of geopolymers synthesized from the RM and metakaolin mixture is in a range of 4–20 MPa [4], while that of geopolymers derived from the RM and fly ash mixture is in a range of 7–13 MPa [1]. In this work, the σ_f of the studied RM–RHA geopolymers ranges from 3.2 to 20.5 MPa, even without the addition of sodium silicate, which is believed to improve the mechanical properties [59]. Thus, the strength of the RM–RHA geopolymers is very competitive and attractive, which is also comparable to that of all types of Portland cement with strengths of 9–20.7 MPa, except the Type III with a strength of 24.1 MPa [40]. As such, they can be used as a cementitious material to replace Portland cement in certain civil engineering applications, such as roadway construction, building materials. In addition, the hematite in the RM–RHA geopolymer composites is actually highly absorptive for heavy metals [54], which can act as a reactive sorbent to filter certain contaminants percolating through the geopolymer composites. Moreover, pure geopolymer binders have the ability to immobilize toxic chemicals and radioactive wastes within their own structures [20,60]. In this regard, the RM–RHA geopolymer can also be used for waste containment and capsulation. It should be expected that the utilization of the RM–RHA geopolymers can bring both environmental and economic advantages. First, geopolymerization of the RM and RHA can save not only the expenses for waste disposal, but also the costs for manufacturing Portland cements. Second, recycle of the two abundant wastes can minimize their potential damage to the environment and human health. Third, the elimination of Portland cement usage can save the energy associated with cement production and reduce the CO_2 emission caused by firing carbonates [22].

Finally, it is also noteworthy that a few barriers may hinder the widespread, practical applications of this particular type of geopolymer composites. The uncertainty in the raw materials' chemical composition and degree or extent of geopolymerization reactions cannot be avoided, and thus may yield certain variations in the mechanical performance of the final products. In addition, the RM–RHA geopolymers take relatively longer durations (e.g., >35 or even 60 days) to achieve complete curing. Such a long curing duration may restrict their applications to cases where fast strength development is not required or time is not a major concern. Moreover, it appears that uncertainties also exist in the geopolymer microstructure (e.g., the fraction of microvoids and microcracks) and side reactions, which are difficult to quantify and hence to assess quantitatively their influences.

3.10. Other practical concerns

Prior efforts were made to reuse RM in cement production, usually in conjunction with other materials, including activators and pozzolans. A recent review by Liu and Zhang [61] summarized the three paths for the utilization of RM as a source for cementitious materials production: use as a raw material to produce cement clinker [7,8], mix with other cementitious or pozzolanic materials to make composite cements [62], and mix with other pozzolanic materials and alkaline activators to make composite cements [63,64]. However, compared with the geopolymerization technique described here, these methods for cement production require high-temperature firing or the use of existing cementitious materials. Moreover, the major binder in the final cured products is still calcium silicate hydrate (C–S–H), and hence some practical concerns with the durability of traditional Portland cement-based concrete are also applicable to the aforementioned RM-based cementitious materials. This is indeed one of the innovative aspects of the geopolymer technology discussed in this paper.

Durability is also a very important factor affecting the structural integrity of cementitious materials. Although durability is not a focus of this study, findings from prior research can shed light on the durability of this particular type of RM–RHA geopolymer composites. For Portland cement concrete, alkali-silica reaction (ASR) that occurs between alkali hydroxides and aggregates containing reactive non-crystalline silica leads to the formation of a gel C–S–H that swells as it adsorbs water from the surrounding cement paste or the environment. As such, the ASR causes serious expansion and cracking in concrete that can occur over a long time period. For geopolymer, however, Li et al. [65] reported that no harmful ASR takes place even at an alkali content as high as 12.1%, most likely owing to the fact that alkali is consumed in the geopolymerization reaction. Furthermore, another study by Yip et al. [66] concluded that the formation of C–S–H gel together with the geopolymeric gel only occurs at low alkalinity, and the coexistence of the two phases is not likely unless a substantial amount of reactive calcium sources is present initially. With respect to chlorine penetration, Lee and van Deventer [48] conducted an experimental study to examine the effect of chloride salts on geopolymer durability, and they found that chlorine or chloride salts are detrimental to the two studied geopolymers owing to the hydrolytic attack of the chlorine on the primary aluminosilicate gel. A few recent studies [67,68] also reported the abrasive resistance or tribological behavior of some geopolymers, and their findings agree that geopolymers in general have better abrasion resistance then the Portland cement concretes, and the tribological behavior can be adjusted by adding solid lubricants (e.g., graphite, molybdenum disulfide) and furnace slag. With respect to carbonation, which is a slow process of forming insoluble calcium carbonate via the reaction between calcium hydroxide and CO_2 in Portland cement concrete, little information is available for geopolymers in the literature. However, it is likely that the CO_2 in air can react with the extra or unreacted NaOH in the geopolymer to form Na_2CO_3. The influence of soluble Na_2CO_3 on the mechanical and microstructural performance of geopolymers is unclear. Nevertheless, according to a recent study by Lee and van Deventer [48], carbonate salts (e.g., K_2CO_3, $CaCO_3$) can be beneficial to geopolymers by lowering the dissolved water contents and preventing hydrolytic attacks on the geopolymer gels. Therefore, it is reasonable to conclude, because of similarity between K_2CO_3 and Na_2CO_3, carbonation in geopolymer may be beneficial to the durability of geopolymers. Finally, the resistance of geopolymers to acid and sulfate attack was investigated by Bakharev [69,70], and it was found that geopolymers' resistance to acid attack was superior to Portland cement paste. Another study by Chindaprasirt et al. [11] showed that blended cements containing fly ash and RHA could enhance the sulfate resistance of Portland cements. In conclusion, based on the limited information available in the literature, geopolymers are expected to possess better durability than Portland cements. More extensive studies are warranted in the future to gain a comprehensive understanding of the durability of geopolymers.

4. Conclusions

This paper presents an experimental study that aimed to convert two industrial wastes, red mud (RM) and rice husk ash (RHA), to a potentially useful construction material via geopolymerization, resulting in a new type of RM–RHA geopolymer composites. The only non-waste material used in the synthesis was NaOH. The amorphous silica in the RHA after dissolution was used as an alternative to the activator, sodium silicate. A variety of synthesis parameters, including curing duration, RHA/RM ratio, RHA particle size, and alkalinity, were examined to understand the extent and degree of geopolymerization and their influence on the

mechanical properties of the final products. The composition and microstructure of the end products were also characterized by X-ray diffraction, electron microscopy, and chemical analysis. Based on the experimental results and observations, the following conclusions can be drawn:

- The synthesized RM–RHA geopolymers are a kind of composite consisting of pure geopolymer binders and other phases as fillers.
- The mechanical properties of the RM–RHA geopolymers are highly complex and dependent upon an array of factors, such as alkalinity, raw material mix ratio, curing duration, RHA particle size, and uncertainties involving incomplete geopolymerization and side reactions.
- The studied geopolymers have compressive strengths of up to 20.5 MPa, which is comparable to most Portland cements, suggesting that the RM–RHA geopolymers can be a potential cementitious construction material.
- A few barriers, such as long curing duration, variability in the raw materials' composition, and uncertainty in the degree of geopolymerization reactions and other side reactions, may cause difficulty in the widespread, practical applications of this kind of geopolymer.

This potential technology, if proved successful, can generate significant environmental and economic impacts to the construction, manufacturing, and energy industries.

Acknowledgments

This study was primarily funded by Grants from the Louisiana Board of Regents ITRS Program, National Basic Research Program of China (2010CB732103), and State Key Laboratory of Hydroscience and Engineering Project (2012-KY-02). The technical support from Charles Skoda and Charles L. Preston of Noranda Alumina, LLC, is gratefully acknowledged. This firm also provided the red mud samples to this study. Jian He received the LSU Graduate School's Enhancement Award to partially support his study.

References

[1] Zhang G, He JA, Gambrell RP. Synthesis, characterization, and mechanical properties of red mud-based geopolymers. Trans Res Record 2010;2167:1–9.
[2] Sahu RC, Patel RK, Ray BC. Neutralization of red mud using CO(2) sequestration cycle. J Hazard Mater 2010;179(1–3):28–34.
[3] Cundi W, Hirano Y, Terai T, Vallepu R, Mikuni A, Ikeda K. Preparation of geopolymeric monoliths from red mud-PFBC ash fillers at ambient temperature. In: Davidovits J, editor. Geopolymer, green chemistry and sustainable development solutions. Saint-Quentin, France: Geopolymer Institute; 2005. p. 85–7.
[4] Dimas DD, Giannopoulou IP, Panias D. Utilization of alumina red mud for synthesis of inorganic polymeric materials. Miner Process Extr Metall Rev 2009;30(3):211–39.
[5] Ayres RU, Holmberg J, Andersson B. Materials and the global environment: waste mining in the 21st century. MRS Bull 2001;26(6):477–80.
[6] Marabini AM, Plescia P, Maccari D, Burragato F, Pelino M. New materials from industrial and mining wastes: glass-ceramics and glass- and rock-wool fibre. Int J Miner Process 1998;53(1–2):121–34.
[7] Singh M, Upadhayay SN, Prasad PM. Preparation of special cements from red mud. Waste Manage 1996;16(8):665–70.
[8] Singh M, Upadhayay SN, Prasad PM. Preparation of iron rich cements using red mud. Cem Concr Res 1997;27(7):1037–46.
[9] Yalcin N, Sevinc V. Utilization of bauxite waste in ceramic glazes. Ceram Int 2000;26(5):485–93.
[10] Chindaprasirt P, Homwuttiwong S, Jaturapitakkul C. Strength and water permeability of concrete containing palm oil fuel ash and rice husk-bark ash. Construct Build Mater 2007;21(7):1492–9.
[11] Chindaprasirt P, Kanchanda P, Sathonsaowaphak A, Cao HT. Sulfate resistance of blended cements containing fly ash and rice husk ash. Construct Build Mater 2007;21(6):1356–61.
[12] Chaudhary DS, Jollands MC. Characterization of rice hull ash. J Appl Polym Sci 2004;93(1):1–8.
[13] Chaudhary DS, Jollands MC, Cser F. Recycling rice hull ash: a filler material for polymeric composites? Adv Polym Technol 2004;23(2):147–55.
[14] Muthadhi A, Anitha R, Kothandaraman S. Rice husk ash – properties and its uses: a review. J Inst Eng 2007;88:55–6.
[15] Songpiriyakij S, Kubprasit T, Jaturapitakkul C, Chindaprasirt P. Compressive strength and degree of reaction of biomass- and fly ash-based geopolymer. Constr Build Mater 2010;24(3):236–40.
[16] Pech-Canul MI, Escalera-Lozano R, Montoya-Davila MA, Pech-Canul M. The use of fly-ash and rice-hull-ash in Al/SiCp composites: a comparative study of the corrosion and mechanical behavior. Materia 2010;15(2):231–9.
[17] Asavapisit S, Ruengrit N. The role of RHA-blended cement in stabilizing metal-containing wastes. Cem Concr Compos 2005;27(7–8):782–7.
[18] Basha EA, Hashim R, Mahmud HB, Muntohar AS. Stabilization of residual soil with rice husk ash and cement. Constr Build Mater 2005;19(6):448–53.
[19] Da Costa HM, Visconte LLY, Nunes RCR, Furtado CRG. The effect of coupling agent and chemical treatment on rice husk ash-filled natural rubber composites. J Appl Polym Sci 2000;76(7):1019–27.
[20] Hart RD, Lowe JL, Southam DC, Perera DS, Wal P. Aluminosilicate inorganic polymers from waste materials. Green Processing 2006, Newcastle, Australia; 2006.
[21] Davidovits J. Geopolymers and geopolymeric materials. J Therm Anal 1989;35(2):429–41.
[22] Davidovits J. Geopolymers – inorganic polymeric new materials. J Therm Anal 1991;37(8):1633–56.
[23] Duxson P, Fernandez-Jimenez A, Provis JL, Lukey GC, Palomo A, van Deventer JSJ. Geopolymer technology: the current state of the art. J Mater Sci 2007;42(9):2917–33.
[24] Komnitsas K, Zaharaki D. Geopolymerisation: a review and prospects for the minerals industry. Miner Eng 2007;20(14):1261–77.
[25] Palomo A, Grutzeck MW, Blanco MT. Alkali-activated fly ashes – a cement for the future. Cem Concr Res 1999;29(8):1323–9.
[26] Xu H, Van Deventer JSJ. The geopolymerisation of alumino-silicate minerals. Int J Miner Process 2000;59(3):247–66.
[27] Allahverdi A, Mehrpour K, Kani EN. Investigating the possibility of utilizing pumice-type natural pozzonal in production of geopolymer cement. Ceram-Silik 2008;52(1):16–23.
[28] Verdolotti L, Iannace S, Lavorgna M, Lamanna R. Geopolymerization reaction to consolidate incoherent pozzolanic soil. J Mater Sci 2008;43(3):865–73.
[29] He J, Zhang G, Hou SA, Cai CS. Geopolymer-based smart adhesives for infrastructure health monitoring: concept and feasibility. J Mater Civ Eng 2011;23(2):100–9.
[30] Latella BA, Perera DS, Durce D, Mehrtens EG, Davis J. Mechanical properties of metakaolin-based geopolymers with molar ratios of Si/Al approximate to 2 and Na/Al approximate to 1. J Mater Sci 2008;43(8):2693–9.
[31] Steveson M, Sagoe-Crentsil K. Relationships between composition, structure and strength of inorganic polymers – Part I – metakaolin-derived inorganic polymers. J Mater Sci 2005;40(8):2023–36.
[32] Steveson M, Sagoe-Crentsil K. Relationships between composition, structure and strength of inorganic polymers – Part 2 – flyash-derived inorganic polymers. J Mater Sci 2005;40(16):4247–59.
[33] Rattanasak U, Chindaprasirt P. Influence of NaOH solution on the synthesis of fly ash geopolymer. Miner Eng 2009;22(12):1073–8.
[34] Cheng TW, Chiu JP. Fire-resistant geopolymer produced by granulated blast furnace slag. Miner Eng 2003;16(3):205–10.
[35] Zhang YS, Sun W, Chen QL, Chen L. Synthesis and heavy metal immobilization behaviors of slag based geopolymer. J Hazard Mater 2007;143(1–2):206–13.
[36] van Jaarsveld JGS, van Deventer JSJ, Lukey GC. The effect of composition and temperature on the properties of fly ash- and kaolinite-based geopolymers. Chem Eng J 2002;89(1–3):63–73.
[37] Kong DL, Sanjayan JG, Sagoe-Crentsil K. Comparative performance of geopolymers made with metakaolin and fly ash after exposure to elevated temperatures. Cem Concr Res 2007;37(12):1583–9.
[38] Swanepoel JC, Strydom CA. Utilisation of fly ash in a geopolymeric material. Appl Geochem 2002;17(8):1143–8.
[39] van Jaarsveld JGS, van Deventer JSJ. Effect of the alkali metal activator on the properties of fly ash-based geopolymers. Ind Eng Chem Res 1999;38(10):3932–41.
[40] ASTM. Annual Book of ASTM Standards; 2010.
[41] Xu H, van Deventer JSJ. Effect of source materials on geopolymerization. Ind Eng Chem Res 2003;42(8):1698–706.
[42] de Jong BHWS, Brown Jr GE. Polymerization of silicate and aluminate tetrahedra in glasses, melts, and aqueous solutions – I. Electronic structure of H6Si2O7, H6AlSiO71- and H6Al2O72-. Geochim Cosmochim Acta 1980;44(3):491–511.
[43] Duxson P, Provis JL, Lukey GC, Mallicoat SW, Kriven WM, van Deventer JSJ. Understanding the relationship between geopolymer composition, microstructure and mechanical properties. Colloid Surf A – Physicochem Eng Asp 2005;269(1–3):47–58.
[44] Chindaprasirt P, Jaturapitakkul C, Chalee W, Rattanasak U. Comparative study on the characteristics of fly ash and bottom ash geopolymers. Waste Manage 2009;29(2):539–43.
[45] Rahier H, Denayer JF, Van Mele B. Low-temperature synthesized aluminosilicate glasses – Part IV – modulated DSC study on the effect of particle size of metakaolinite on the production of inorganic polymer glasses. J Mater Sci 2003;38(14):3131–6.

[46] Somna K, Jaturapitakkul C, Kajitvichyanukul P, Chindaprasirt P. NaOH-activated ground fly ash geopolymer cured at ambient temperature. Fuel 2011;90(6):2118–24.
[47] Hardjito D, Wallah SE, Sumajouw DMJ, Rangan BV. On the development of fly ash-based geopolymer concrete. ACI Mater J 2004;101(6):467–72.
[48] Lee WKW, van Deventer JSJ. The effects of inorganic salt contamination on the strength and durability of geopolymers. Colloid Surf A – Physicochem Eng Asp 2002;211(2–3):115–26.
[49] Shen JF, Liu XZ, Zhu SG, Zhang HL, Tan JJ. Effects of calcination parameters on the silica phase of original and leached rice husk ash. Mater Lett 2011;65(8):1179–83.
[50] Shinohara Y, Kohyama N. Quantitative analysis of tridymite and cristobalite crystallized in rice husk ash by heating. Ind Health 2004;42(2):277–85.
[51] Foo KY, Hameed BH. Utilization of rice husk ash as novel adsorbent: a judicious recycling of the colloidal agricultural waste. Adv Colloid Interface Sci 2009;152(1–2):39–47.
[52] He J, Zhang J, Yu Y, Zhang G. The strength and microstructure of two geopolymers derived from metakaolin and red mud-fly ash admixture: a comparative study. Constr Build Mater 2012;30:80–91.
[53] Lecomte I, Liegeois M, Rulmont A, Cloots R, Maseri F. Synthesis and characterization of new inorganic polymeric composites based on kaolin or white clay and on ground-granulated blast furnace slag. J Mater Res 2003;18(11):2571–9.
[54] Schwertmann U, Taylo RM. Iron oxides. In: Dixon JB, Weed SB, editors. Minerals in soil environments. Madison, WI: Soil Science Society of America; 1989. p. 379–465.
[55] Zivica V, Balkovic S, Drabik M. Properties of metakaolin geopolymer hardened paste prepared by high-pressure compaction. Constr Build Mater 2011;25(5):2206–13.
[56] Aly Z, Vance ER, Perera DS, Hanna JV, Griffith CS, Davis J, et al. Aqueous leachability of metakaolin-based geopolymers with molar ratios of Si/Al = 1.5 − 4. J Nucl Mater 2008;378(2):172–9.
[57] Bell JL, Driemeyer PE, Kriven WM. Formation of ceramics from metakaolin-based geopolymers. Part II: K-based geopolymer. J Am Ceram Soc 2009;92(3):607–15.
[58] van Jaarsveld JGS, van Deventer JSJ, Lukey GC. The characterisation of source materials in fly ash-based geopolymers. Mater Lett 2003;57(7):1272–80.
[59] Zhang B, MacKenzie KJD, Brown IWM. Crystalline phase formation in metakaolinite geopolymers activated with NaOH and sodium silicate. J Mater Sci 2009;44(17):4668–76.
[60] Van Jaarsveld JGS, Van Deventer JSJ, Lorenzen L. The potential use of geopolymeric materials to immobilise toxic metals: Part I. Theory Appl Miner Eng 1997;10(7):659–69.
[61] Liu XM, Zhang N. Utilization of red mud in cement production: a review. Waste Manage Res 2011;29(10):1053–63.
[62] Zhang N, Liu XM, Sun HH, Li LT. Evaluation of blends bauxite-calcination-method red mud with other industrial wastes as a cementitious material: properties and hydration characteristics. J Hazard Mater 2011;185(1):329–35.
[63] Pan ZH, Cheng L, Lu YN, Yang NR. Hydration products of alkali-activated slag-red mud cementitious material. Cem Concr Res 2002;32(3):357–62.
[64] Pan ZH, Li DX, Yu J, Yang NR. Properties and microstructure of the hardened alkali-activated red mud-slag cementitious material. Cem Concr Res 2003;33(9):1437–41.
[65] Li KL, Huang GH, Jiang LH, Cai YB, Chen J, Ding JT. Study on abilities of mineral admixtures and geopolymer to restrain ASR. In: Feng NQ, Peng GF, editors. Environmental ecology and technology of concrete. Zurich-Uetikon: Trans Tech Publications Ltd.; 2006. p. 248–54.
[66] Yip CK, Lukey GC, van Deventer JSJ. The coexistence of geopolymeric gel and calcium silicate hydrate at the early stage of alkaline activation. Cem Concr Res 2005;35(9):1688–97.
[67] Hu SG, Wang HX, Zhang GZ, Ding QJ. Bonding and abrasion resistance of geopolymeric repair material made with steel slag. Cem Concr Compos 2008;30(3):239–44.
[68] Wang HL, Li HH, Yan FY. Synthesis and tribological behavior of metakaolinite-based geopolymer composites. Mater Lett 2005;59(29–30):3976–81.
[69] Bakharev T. Durability of geopolymer materials in sodium and magnesium sulfate solutions. Cem Concr Res 2005;35(6):1233–46.
[70] Bakharev T. Resistance of geopolymer materials to acid attack. Cem Concr Res 2005;35(4):658–70.